Glutathione peroxidase 4 and vitamin E control reticulocyte maturation, stress erythropoiesis and iron homeostasis

Sandro Altamura,[1,2,*] Naidu M. Vegi,[3*] Philipp S. Hoppe,[4] Timm Schroeder,[4] Michaela Aichler,[5] Axel Walch,[5] Katarzyna Okreglicka,[6] Lothar Hültner,[7] Manuela Schneider,[8] Camilla Ladinig,[7] Cornelia Kuklik-Roos,[7] Josef Mysliwietz,[9] Dirk Janik,[5] Frauke Neff,[5] Birgit Rathkolb,[10-12] Martin Hrabé de Angelis,[11-13] Christian Buske,[3] Ana Rita da Silva,[1,2] Katja Muedder,[1,2] Marcus Conrad,[14] Tomas Ganz,[15] Manfred Kopf,[6] Martina U. Muckenthaler[1,2] and Georg W. Bornkamm[7,#]

These authors contributed equally to this work

[1]Department of Pediatric Hematology, Oncology and Immunology - University of Heidelberg, Heidelberg, Germany; [2]Molecular Medicine Partnership Unit, Heidelberg, Germany; [3]Institute of Experimental Cancer Research, Universitätsklinikum Ulm, Ulm, Germany; [4]Department of Biosystems Bioscience and Engineering, ETH Zürich, Basel, Switzerland; [5]Research Unit Analytical Pathology, Helmholtz Zentrum München, Deutsches Forschungszentrum für Gesundheit und Umwelt (GmbH), Neuherberg, Germany; [6]Institute of Molecular Health Sciences, ETH Zurich, Zürich, Switzerland; [7]Institute of Clinical Molecular Biology and Tumor Genetics, Helmholtz Zentrum München, Deutsches Forschungszentrum für Gesundheit und Umwelt (GmbH), München, Germany; [8]Institute for Stroke and Dementia Research (ISD), Klinikum der Universität München, München, Germany; [9]Institute of Molecular Immunology, Helmholtz Zentrum München, Deutsches Forschungszentrum für Gesundheit und Umwelt (GmbH), München, Germany; [10]Institute of Molecular Animal Breeding and Biotechnology, Ludwig-Maximilians-Universität München, Genzentum, München, Germany; [11]Institute of Experimental Genetics, Geman Mouse Clinic (GMC), Helmholtz Zentrum München, Deutsches Forschungszentrum für Gesundheit und Umwelt (GmbH), Neuherberg, Germany; [12]German Center for Diabetes Research (DZD), Neuherberg, Germany; [13]Chair of Experimental Genetics, School of Life Science Weihenstephan, Technische Universität München, Freising, Germany; [14]Institute of Developmental Genetics, Helmholtz Zentrum München, Deutsches Forschungszentrum für Gesundheit und Umwelt (GmbH), Neuherberg, Germany and [15]Departments of Medicine and Pathology, David Geffen School of Medicine, UCLA, Los Angeles, CA, USA

 doi:10.3324/haematol.2018.212977

Received: November 24, 2018.

Accepted: June 20, 2019.

Pre-published: June 27, 2019.

Correspondence: *GEORG W. BORNKAMM* - georg.bornkamm@t-online.de

Supplementary Information

Antibodies for FACS analysis

Antigen-Conjugate	Company	Clone	Concentration
CD44-PE-Cy7	eBiosciences	IM7	0.3µg/50µL
CD71-PE-Cy7	Biolegend	R17217	0.3µg/50µL
Ter119-PE	eBiosciences	Ter119	0.3µg/50µL
Ter119-APC-Cy7	eBiosciences	Ter119	0.3µg/50µL
CD16/32	BD Biosciences	2.4G2	0.5µg/50µL
CD3e-biotin	eBiosciences	145-2C11	0.5µg/50µL
CD11b-biotin	eBiosciences	M1/70	0.5µg/50µL
CD19-biotin	eBiosciences	1D3	0.5µg/50µL
B220-biotin	eBiosciences	RA3-682	0.5µg/50µL
GR-1-biotin	eBiosciences	RB5-8C5	0.5µg/50µL
CD45-BV785	Biolegend	30-F11	0.01µg/50µL
CD11b-PerCP-Cy5.5	Biolegend	M1/70	0.01µg/50µL
F4/80-BV421	Biolegend	BM8	0.08µg/50µL
CD11c-BV605	Biolegend	N418	0.02µg/50µL
VCAM1-FITC	eBiosciences	429	0.125µg/50µL
MHCII-BV510	Biolegend	M5/114.15.2	0.06µg/50µL
Ly6C-APC	Biolegend	HK1.4	0.005µg/50µL

Antibodies for Western-blotting

Protein	Company	Cat nr	Dilution
GPX4	ABCAM	125066	1:1000
Fpn	Alpha Diagnostics	MTP11-A	1:1000
HO1	Enzo Life Sciences	ADI-SPA-896-F	1:500
FtL	Santa Cruz	sc-14420	1:250
Actin	Sigma	A1978	1:10000

Primers for monitoring deletion of the GPX4 gene

	Primer forward	Primer reverse
floxed vs wt	ACTCCCCGTGGAACTGTGAGCTTTGTGC	GGATCTAAGGATCACCAGAGCTGAGGCTGC
deleted	GTGTACCACGTAGGTACAGTGTCTGC	GGATCTAAGGATCACCAGAGCTGAGGCTGC

Primers for quantitative RT-PCR

	Primer forward	Primer reverse
GPX4	CGCTCCATGCACGAATTCTC	GCACACGAAACCCCTGTACT
Fpn	TGTCAGCCTGCTGTTTGCAGGA	TCTTGCAGCAACTGTGTCACCG
Hepcidin	ATACCAATGCAGAAGAGAAGG	AACAGATACCACACTGGGAA
SMAD6	GTTGCAACCCCACTTC	GGAGGAGACAAGAATA
SMAD7	GCAGGCTGTCCAGATGCTGT	GATCCCCAGGCTCCAGAAGA
ID1	ACCCTGAACGGCGAGATCA	TCGTCGGCTGGAACACATG
HO-1	AGGCTAAGACCGCCTTCCT	TGTGTTCCTCTGTCAGCATCA
Erfe	AGCGAGCTCTTCACCATCTC	TGTCCAAGAAGACAGAAGTGTAGTG
RPL19	AGGCATATGGGCATAGGGAAGAG	TTGACCTTCAGGTACAGGCTGTG
Fpn	TGTCAGCCTGCTGTTTGCAGGA	TCTTGCAGCAACTGTGTCACCG
Hepcidin	ATACCAATGCAGAAGAGAAGG	AACAGATACCACACTGGGAA
SMAD6	GTTGCAACCCCACTTC	GGAGGAGACAAGAATA
SMAD7	GCAGGCTGTCCAGATGCTGT	GATCCCCAGGCTCCAGAAGA
ID1	ACCCTGAACGGCGAGATCA	TCGTCGGCTGGAACACATG
HO-1	AGGCTAAGACCGCCTTCCT	TGTGTTCCTCTGTCAGCATCA
Erfe	AGCGAGCTCTTCACCATCTC	TGTCCAAGAAGACAGAAGTGTAGTG
RPL19	AGGCATATGGGCATAGGGAAGAG	TTGACCTTCAGGTACAGGCTGTG

Staining of spleen red pulp macrophages (RPM) and bone marrow erythroblastic island macrophages (BMEIM) in GPX4$^{fl/fl}$;LysM-Cre mice

Spleens were cut into small pieces, then digested for 30 min at 37 °C with 2 mg/ml of type IV collagenase (Worthington) and 50U/ml DNase I (Sigma) and passed through a 70-µm cell strainer. Bone marrow was flushed from femur and tibia from mouse hindlimb and passed through a 70-µm cell strainer. Erythrocytes were lysed with ACK (ammonium chloride–potassium bicarbonate) buffer. Dead cells were gated out with use of the live-dead marker eFluor780 (eBioscience). FcγIII/II receptors were blocked by incubation with anti-CD16/32 antibody for 15 min on ice. Cells were washed and incubated with 0.01µg CD45-BV785, 0.01µg CD11b-PerCP-Cy5.5, 0.08µg F4/80-BV421, 0.02µg CD11c-BV605, 0.125µg VCAM1-FITC, 0.06µg MHCII-BV510, and 0.005µg Ly6C-APC antibodies. Cells were analysed on LSR Fortessa (Becton Dickinson).

Transmission Electron microscopy

Blood pellets were fixed in 2.5% electron microscopy grade glutaraldehyde in 0.1 M sodium cacodylate buffer pH 7.4 (Science Services, Munich, Germany), postfixed in 2% aqueous osmium tetraoxide,[1] dehydrated in gradual ethanol (30–100%) and propylene oxide, embedded in Epon (Merck, Darmstadt, Germany) and cured for 24 hours at 60°C. Semithin sections were cut and stained with toluidine blue. Ultrathin sections of 50 nm were collected onto 200 mesh copper grids, stained with uranyl acetate and lead citrate before examination by transmission electron microscopy (Zeiss Libra 120 Plus, Carl Zeiss NTS GmbH, Oberkochen, Germany). Pictures were acquired using a Slow Scan CCD-camera and iTEM software (Olympus Soft Imaging Solutions, Münster, Germany).

Determining the maturation state of reticulocytes

Peripheral blood cells were washed with PBS containing 1 mM EDTA and 2% FCS, filtered through a 40 µm cell strainer (BD Falcon) and incubated with 0.5 µg anti-CD16/32 antibody (clone 2.4G2, BD Bioscience) in 50 µl PBS for 30 min on ice. Cells were stained with 0.3 µg CD71-PE-Cy7, 0.3 µg Ter119-PE or Ter119-APC-Cy7 antibodies for another 30 minutes as well as with Mitotracker Deep Red (MTDR) (Thermo Fisher) and Thiazol Orange (TO)(Biomol) in 50 µL PBS according to the manufacturer's instructions. Mature reticulocytes are defined by CD71 and Ter119 staining as enucleated CD71^{low}/Ter119^{high} cells. CD71^{high}/TEr119^{high} reticulocytes are divided into immature and highly immature reticulocytes based on MTDR and TO staining.

Determining the total number of proerythroblasts and erythroblasts in the bone marrow and spleen and of erythrocytes and reticulocytes in the blood

The percentual fractions of proerythroblasts ($CD71^{high}$, $Ter119^{low}$) and erythroblasts ($CD71^{high-low}$, $Ter119^{high}$) in the bone marrow and spleen were determined by FACS analysis as exemplified in Fig.2. Based on the percentual fractions the total number of erythroid precursors in the bone marrow was assessed by counting absolute cell numbers in the four hindlimb bones and extrapolating the values obtained from wt mice to the known bone marrow cellularity of adult female C57BL/6 wt mice ($466x10^6$ cells).[2] The total number of erythroid precursor cells in the spleen was calculated based on the percentual fraction of erythroid precursor cells in the spleen and the assumption that 100 mg spleen tissue contains 10^8 nucleated cells. The total number of erythrocytes and reticulocytes was assessed based on the fact that 7.8 to 8.0% of the body weight of adult female C57BL/6 mice is blood.[3]

Histology

Histology was done following standard procedures.[4] Immunohistochemistry was performed in a Ventana immunostainer from Roche diagnostics according to manufacturer's instructions.

Western-blot

Protein lysates were obtained by homogenizing snap-frozen tissues in RIPA or LCW buffer supplemented with protease and phosphatase inhibitors (Roche).[5] Protein concentration was determined using the DC protein assay (BioRad). 50µg of total protein and β-actin (Actin) as normalizer were subjected to Western-blot analysis. Western-blot images were acquired on X-ray films and different exposures scanned for quantification.

Genomic DNA PCR, RNA Extraction, reverse transcription and qRT-PCR

Deletion of the *GPX4* gene was analysed using two PCR reactions: the first reaction (primer pair oligoGPX4I5f1/ oligoPFrev1, annealing 65.5°C, elongation for 60 sec) detects the deleted allele (509 bp), whereas the second reaction (primer pair oligoPFf1/oligoPFrev1, annealing 68°C, elongation 30 sec) discriminates between the floxed (262 bp) and the wt allele (178 bp). Both PCR reactions were pooled for gel electrophoresis. Incomplete deletion of *GPX4* is detected by the presence of the floxed allele. RNA was isolated from tissues using the Trizol reagent (Life technologies) and TissueLyser homogenizer (Qiagen), reverse-transcribed and used in SYBR green qRT-PCR as described.[6] mRNA expression was calculated relative to RPL19. Data were analyzed using the ΔΔCt method.[7]

Plasma and liver biochemistry and tissue iron measurement

Plasma iron concentration was assessed using the SFBC colorimetric kit (Biolabo, Maizy, France). Plasma ferritine and bilirubin were measured using the Olympus AU400 analyzer at the Claude Bernard Institute (Paris, France). Tissue non-heme iron content was measured using the bathophenanthroline method and calculated against dry weight tissue.[8] Hepatic lipid peroxidation was assessed on 0.05g hepatic tissue using the thiobarbituric acid assay (TBARS).[9]

Plasma hepcidin, erythropoietin (EPO) and erythroferrone (ERFE) measurement

Plasma hepcidin and EPO concentrations were measured using the "Hepcidin Murine-Compete ELISA Kit" (Intrinsic Lifescience, USA) and the "Mouse erythropoietin quantikine ELISA kit" (R&D systems) according to manufacturer's instructions. Mouse ERFE was measured in a custom ELISA using monoclonal antibodies and recombinant mouse ERFE standards, kindly donated by Silarus Therapeutics (La Jolla, CA, USA), as described.[10] Concentrations were extrapolated against a standard curve using the GraphPad Prism software.

Statistical analyses

Figures were generated and statistical analyses performed by using GraphPad Prism software (Version 6.01 for Windows). Normality test (Shapiro-Wilk test) and Bartlett's test of homogeneity variances and two-way ANOVA with no assumption of homogeneity of variance (with Sidak's test of multiple comparisons) were used to calculate statistical significances unless otherwise stated in the figure legends. Differences with p values less than 0.05 were considered to be statistically significant (* $p<0.05$; ** $p<0.001$; *** $p<0.0001$; **** $p<0.0001$). Values mentioned are Mean ± SEM.

Legends to Supplementary Figures

Supplementary Figure 1:

Cre activation induces an aplastic anemia in mice with *GPX4*-deficient as well as *GPX4*-proficient hematopoietic system. Scheme of the wt and gene-modified murine GPX4 locus before and after Cre activation. White and black triangles represent loxP and frt sites, respectively (A). Lethally irradiated mice reconstituted with BM cells from *GPX4$^{fl/fl}$;CreERT2* or *GPX4$^{wt/wt}$;CreERT2* donor mice were fed a tamoxifen citrate containing diet for three weeks to delete *GPX4*. EDTA-blood was collected from the tail vein before (left columns, - TAM) and at the last day of tamoxifen administration (right columns, + TAM), and subjected to the analysis of blood parameters (mice harboring *GPX4* in the bone marrow, designated wt, black columns, n=7, and mice lacking *GPX4* in the bone marrow, designated ko, grey columns, n=22). Red blood counts (RBC, B), hemoglobin (HGB, C), hematocrit (HCT,D), mean corpuscular volume (MCV, E) reticulocyte counts (F) , platelet counts (G), mean platelet volume (MPV, H), platelet width distribution (PDW, I), platelet large cell fraction (P-LCR, J), platelet crit (PCT, K), white blood counts (WBC, L), neutrophils (M), lymphocytes (N), monocytes (O), and eosinophils (P) were determined. For reticulocytes (F) and eosinophils (P) that did not pass the Shapiro-Wilk normality test, non-parametric ANOVA with Dunn's multiple comparison test was applied. The decrease in lymphocyte and monocyte counts induced by Cre activation in control mice is further significantly enhanced by *GPX4*-deficiency in the hematopoietic system. The increase in platelet indices PMV, PDW and P-LCR is presumably a transient response to toxic platelet activation.[11]

Supplementary Figure 2:

Additional red blood cell parameters to the experiments shown in Fig. 1D-H and I-M. The temporal schemes in A and F are identical to the schemes in Fig. 1D and I. Mean cell volume (MCV) (B and G), mean cell hemoglobin (MCH) (C and H), mean cell hemoglobin concentration (MCHC) (D and I), and red blood cell distribution width (RDW-SD) (E and J). Number of mice and designations as in Fig.1. MCV, MCH and RDW-SD are significantly increased in mice with a *GPX4*-deficient hematopoietic system. Vitamin E depletion further aggravates the phenotype (G,H,J).

Supplementary Figure 3:

The erythropenic phenotype induced by *GPX4* deficiency in the hematopoietic system is stably transmitted in two consecutive rounds of bone marrow transplantation. Experimental design and temporal scheme (A). Lethally irradiated wt mice were reconstituted with 10^6 BM cells of *GPX4*$^{fl/fl}$*;Cre-ERT2* mice (1st transplantation) and allowed to recover for 12 weeks before a tamoxifen citrate containing diet was administered for three weeks. Three mice of the same 1st transplantation group were not treated with tamoxifen and served as control donors for the 2nd transplantation. Two weeks after terminating the tamoxifen containing diet, 10^6 bone marrow cells of mice that had received the tamoxifen containing diet (grey bars, designated + TAM, n=5) and of control mice that had not received tamoxifen (black bars, designated – TAM, n=5) were injected into lethally irradiated wt mice (2nd transplantation). 20 weeks after the 2nd transplantation, 10^6 *GPX4*-deficient (n=10) and *GPX4*- proficient BM cells (n=6) of the recipients of the 2nd transplantation were injected into lethally irradiated wt mice (3rd transplantation). Blood was drawn 11 weeks after the second and 11 weeks after the third transplantation. The erythropenic phenotype was stably transmitted after deletion of *GPX4* in the hematopoietic system in two consecutive rounds of BM transplantation (2nd and 3rd transplantation)(B, C, D, E, I), whereas alterations in the white blood counts and platelet indices were not consistently observed after the 2nd and 3rd transplantation (J-O).

Supplementary Figure 4:

Minor differences in the development of red pulp and and bone marrow erythroblastic island macrophages in GPX4$^{fl/fl}$;LysM-Cre mice. Representative FACS plots showing gating strategy for red pulp macrophages (RPM, A, n=3) and bone marrow erythroblastic island macrophages (BMEIM, B, n=3) for *GPX4*$^{fl/fl}$*;LysM-Cre* and *GPX*$^{fl/fl}$ mice. Cell counts, frequencies of CD45-positive cells for RPM (upper panel) and BMEIM (lower panel) supplemented with total counts for spleen and bone marrow cells are shown in C. The significance was calculated with unpaired two-tailed Student's t-test.

Supplementary Figure 5:

Erythropoiesis is not affected by vitamin E depletion in wt mice. Three weeks old female wt mice were fed either a normal (black columns, designated + vitE, n=10) or a vitamin E-depleted diet (grey columns, designated – vitE, n=9) upon weaning. Blood was

drawn 17 weeks after starting the vitamin E depleted diet (A). In wt mice red blood parameters were not affected by vitamin E depletion in the diet (B-I).

Supplementary Figure 6:

Reticulocyte maturation is impaired by *GPX4*-deficiency in the hematopoietic system and the phenotype is strongly aggravated by concomitant vitamin E depletion. Total numbers of mature, immature, and highly immature reticulocytes in wt mice maintained on a normal diet (A, n=4) and in mice with *GPX4*-deficient hematopoiesis kept either on a normal (B, n=4) or vitamin E-depleted diet (C, n=6). The FACS staining of blood cells of one representative mouse of each group is shown in Fig. 5A-C. Mature reticulocytes were defined by $CD71^{low}$/$Ter119^{high}$ staining. $CD71^{high}$/$Ter119^{high}$ cells were divided into immature and highly immature reticulocytes based on Mitotracker Deep Red (MTDR) and thiazol orange (TO) staining. The total numbers of reticulocytes of the various stages of maturation were determined based on the percentual fraction of mature, immature and highly immature reticulocytes, the reticulocyte counts per µL obtained by Sysmex analysis, and the mean total blood content (7.8 to 8.0 % of body weight) of adult female C57BL/6 mice.[3] The significance was calculated by Mann-Whitney test. To visualize and quantify the differences in each fraction of reticulocytes under the different conditions, data of A, B, and C were replotted in D, E, and F. Deletion of *GPX4* in hematopoietic cells of mice kept on a normal diet caused an increase in all fractions of reticulocytes (D-F). The differentially higher increase in more immature cells resulted in a general shift towards more immature reticulocytes (G-I). Under combined *GPX4*- and vitamin E-deficiency, production of reticulocytes did not keep up with the severity of the erythropenia and the production of proerythroblasts in the spleen, i.e. total reticulocyte counts were not increased to a significant extent compared to wt mice despite the strong decrease in RBC, hemoglobin and hematocrit. The absolute numbers as well as the percentage of highly immature reticulocytes were increased in these mice at the expense of mature reticulocytes (C,F,I).

Supplementary Figure 7:

Ferroportin expression in the duodenum and hemoxygenase-1 expression in the liver. Unaltered ferroportin (Fpn) expression in mice with GPX4-deficient hematopoiesis (A). Quantification of hemoxygenase-1 expression in the liver of mice with GPX4-deficiency in the hematopoietic system (B).

Supplementary References

1. Wood RL, Luft JH. The Influence of Buffer Systems on Fixation with Osmium Tetroxide. J Ultrastruct Res. 1965;12:22-45.
2. Colvin GA, Lambert JF, Abedi M, et al. Murine marrow cellularity and the concept of stem cell competition: geographic and quantitative determinants in stem cell biology. Leukemia. 2004;18(3):575-583.
3. Harkness JE, American College of Laboratory Animal M. Harkness and Wagner's biology and medicine of rabbits and rodents. Oxford: Wiley-Blackwell, 2010.
4. Suvarna SK. Bancroft's theory and practice of histological techniques / Kim S Suvarna, Christopher Layton, John D. Bancroft. Kidlington: Elsevier, 2018.
5. Ingold I, Berndt C, Schmitt S, et al. Selenium Utilization by GPX4 Is Required to Prevent Hydroperoxide-Induced Ferroptosis. Cell. 2018;172(3):409-422.
6. Altamura S, D'Alessio F, Selle B, Muckenthaler MU. A novel TMPRSS6 mutation that prevents protease auto-activation causes IRIDA. The Biochemical journal. 2010;431(3):363-371.
7. Livak KJ, Schmittgen TD. Analysis of Relative Gene Expression Data Using Real-Time Quantitative PCR and the 2-[Delta][Delta]CT Method. Methods. 2001;25(4):402-408.
8. Torrance JD, Bothwell TH. A simple technique for measuring storage iron concentrations in formalinised liver samples. S Afr J Med Sci. 1968;33(1):9-11.
9. Ohkawa H, Ohishi N, Yagi K. Assay for lipid peroxides in animal tissues by thiobarbituric acid reaction. Analytical biochemistry. 1979;95(2):351-358.
10. Kautz L, Jung G, Du X, et al. Erythroferrone contributes to hepcidin suppression and iron overload in a mouse model of beta-thalassemia. Blood. 2015;126(17):2031-2037.
11. Jindal S, Gupta S, Gupta R, et al. Platelet indices in diabetes mellitus: indicators of diabetic microvascular complications. Hematology. 2011;16(2):86-89.

Supplementary Figure 1

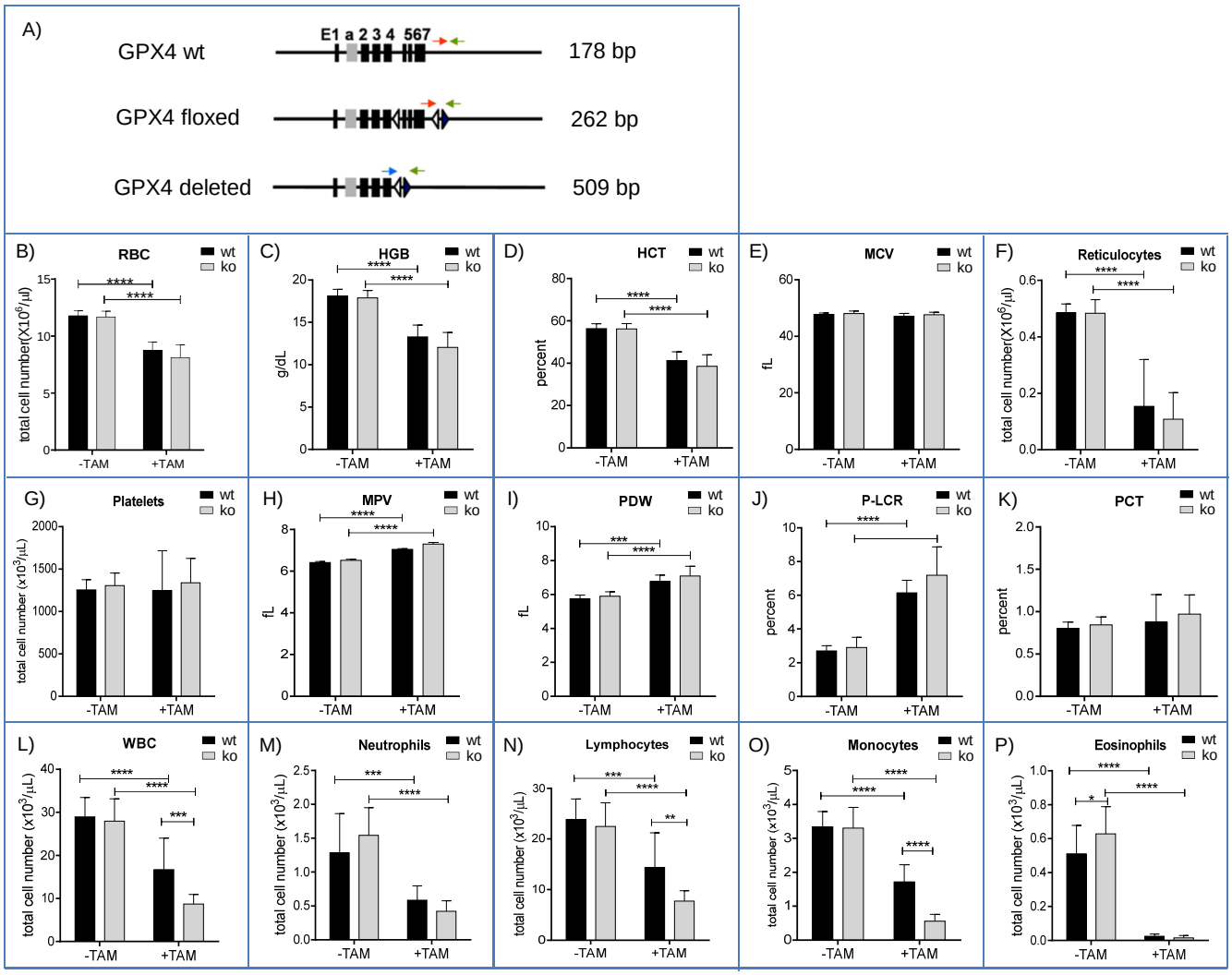

Supplementary Figure 2

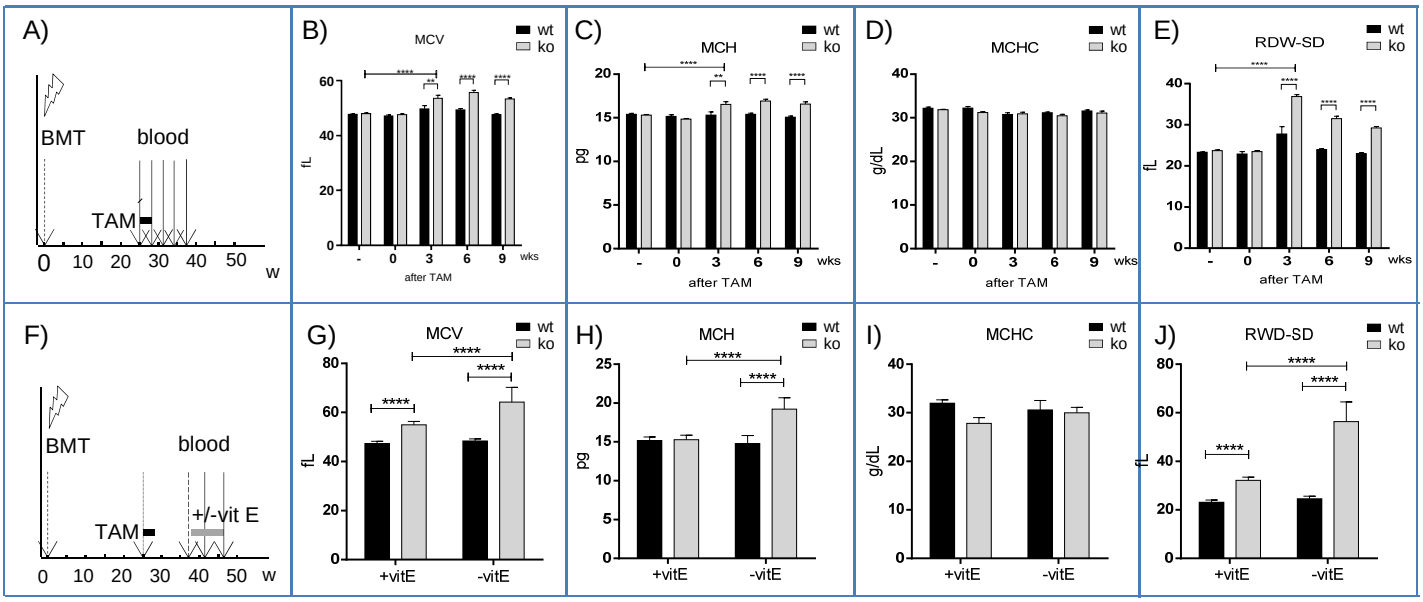

Supplementary Figure 3

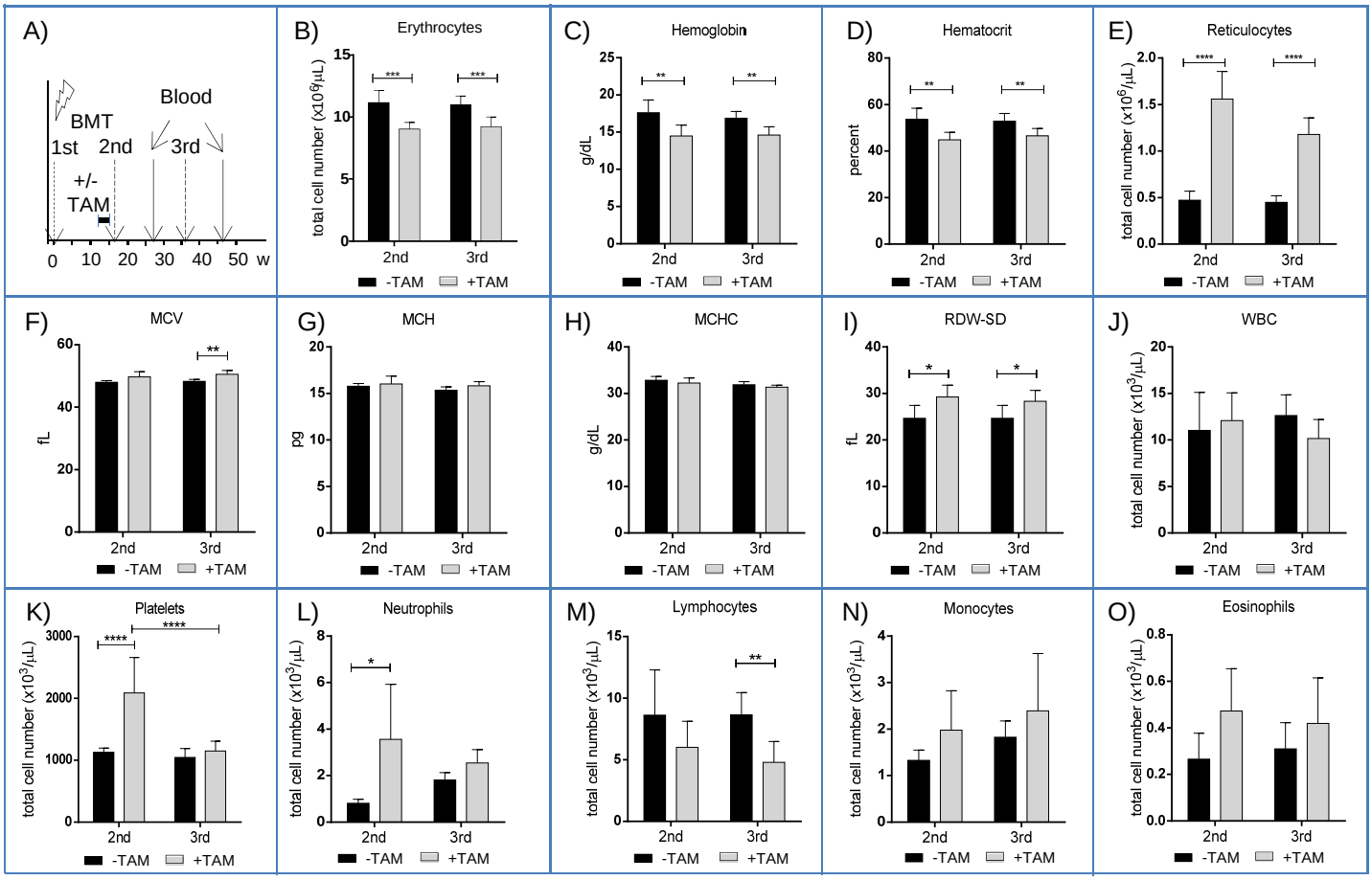

Supplementary Figure 4

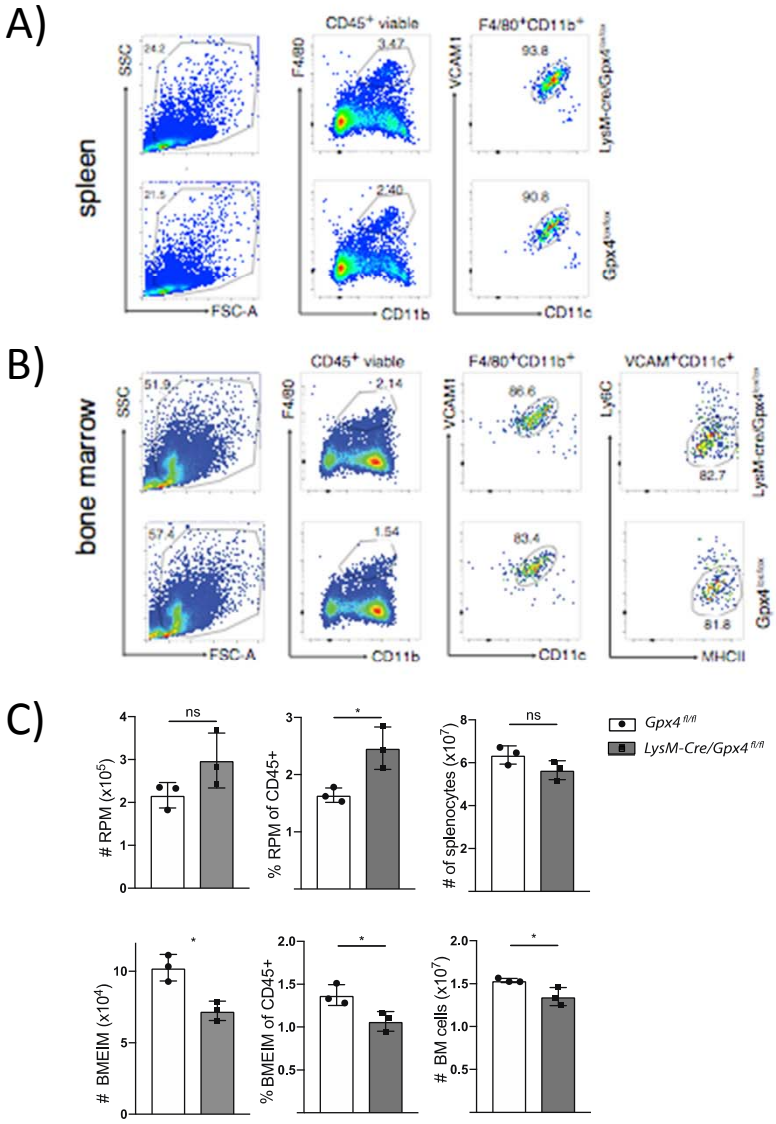

Supplementary Figure 5

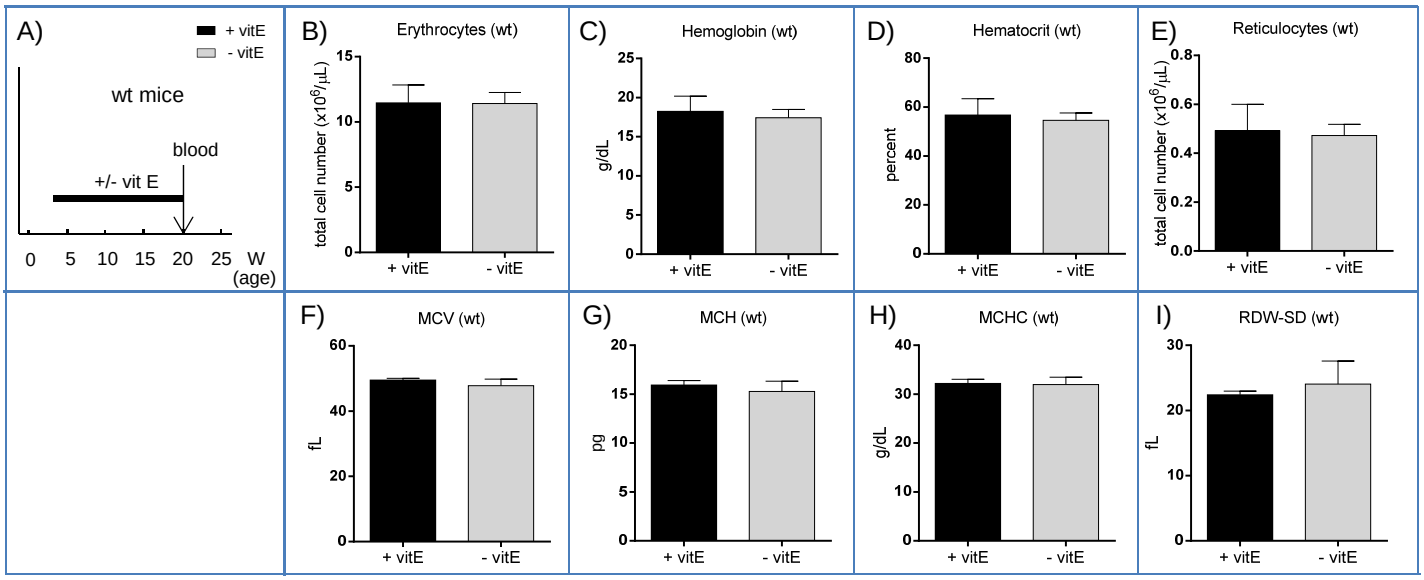

Supplementary Figure 6

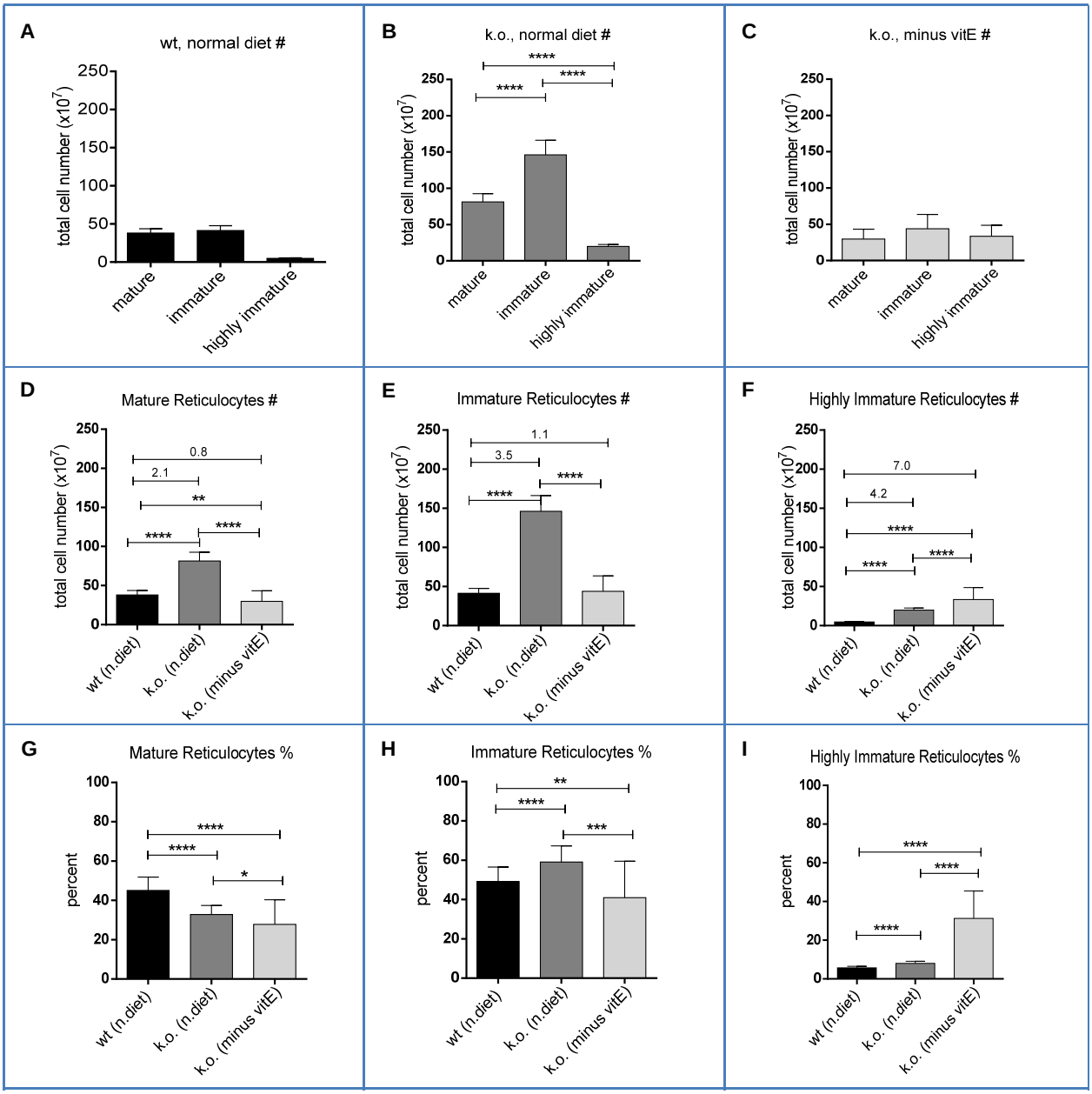

Supplementary Figure 7